Magnetization steps in dilute magnetic semiconductors to 55 T: Mn^{2+} pair saturation in $Cd_{1-x}Mn_xTe$ and steps in $Zn_{1-x}Mn_xSe$, $Zn_{1-x}Mn_xTe$, and $Cd_{1-x}Mn_xSe$

S. Foner
Francis Bitter National Magnet Laboratory and Department of Physics, Massachusetts Institute of Technology, Cambridge, Massachusetts 02139

Y. Shapira
Department of Physics, Tufts University, Medford, Massachusetts 02155

D. Heiman and P. Becla
Francis Bitter National Magnet Laboratory, Massachusetts Institute of Technology, Cambridge, Massachusetts 02139

R. Kershaw, K. Dwight, and A. Wold
Department of Chemistry, Brown University, Providence, Rhode Island 02912
(Received 24 January 1989)

Pulsed-field magnetization measurements in dilute magnetic semiconductors were made up to 55 T at 1.4 K in order to determine the nearest-neighbor antiferromagnetic exchange J_{NN} for Mn^{2+} pairs. For $Cd_{1-x}Mn_xTe$ ($x=0.047$), $J_{NN}/k_B=-6.2\pm0.2$ K. This $|J_{NN}|$ was sufficiently small so that all five predicted "magnetization pair steps" due to pairs were observed with a pulsed-field magnet fabricated with a newly developed Cu/Nb metal-matrix microcomposite conductor. Two magnetization steps were observed in $Zn_{1-x}Mn_xSe$ ($x=0.033$), $Zn_{1-x}Mn_xTe$ ($x=0.031$ and 0.040), and $Cd_{1-x}Mn_xSe$ ($x=0.049$), from which we obtained $J_{NN}/k_B=-12.2\pm0.3$ K, -9.0 ± 0.2 K, and -7.6 ± 0.2 K, respectively.

I. INTRODUCTION

The purpose of this paper is twofold. First, we report the observation of all five steplike increases in magnetization with increasing field (magnetization steps) which are predicted to arise from isolated nearest-neighbor pairs in dilute magnetic semiconductors. This observation was made on $Cd_{1-x}Mn_xTe$, with $x=0.047$. Second, we report values for the nearest-neighbor (NN) Mn-Mn exchange constant in $Zn_{1-x}Mn_xTe$ and $Zn_{1-x}Mn_xSe$, which resolve the discrepancies between earlier results. Our measurements also confirm previously published values for the NN exchange constant in $Cd_{1-x}Mn_xTe$ and $Cd_{1-x}Mn_xSe$.

Dilute magnetic semiconductors (DMS's) are compound semiconductors in which a fraction of the ions are magnetic. The best known group of DMS's are II-VI compounds in which a fraction x of the cations are Mn^{2+}, e.g., $Cd_{1-x}Mn_xTe$. The extensive research on this group of materials, and on other DMS's, has been reviewed recently.[1] One aspect of this research focused on the exchange interactions between the Mn^{2+} ions. This is the *d-d* exchange, as distinguished from the *sp-d* exchange between the spins of the Mn ions and the spins of the electrons and holes near the band edges. An extensive theoretical discussion of both types of exchange interactions was given by Larson, Hass, and Ehrenreich.[2] It was shown that the dominant mechanism for the Mn-Mn exchange is the superexchange. This conclusion is supported by experiment.[3] The theory of Larson *et al.* also indicates that the largest Mn-Mn exchange constant is for Mn ions which occupy nearest-neighbor positions in the cation sublattice. Specifically, $|J_{NN}|$ for NN's is an order of magnitude larger than $|J_{NNN}|$ for next-nearest neighbors. The available experimental data (e.g., Ref. 4) support this conclusion.

Several accurate methods for determining J_{NN} have been developed in the last several years. All these methods probe the energy-level structure of an isolated (or nearly isolated) pair of NN Mn ions. This "pair spectroscopy" leads to values which are in rough agreement with the theory of Larson *et al.* A typical value of J_{NN} in II-VI DMS's containing Mn is $J_{NN}/k_B\sim-10$ K, where k_B is the Boltzmann constant. The negative sign of J_{NN} corresponds to an antiferromagnetic interaction.

In Sec. II the various methods of pair spectroscopy are reviewed with an emphasis on the magnetization-steps method which is employed in this work. The experimental techniques are described in Sec. III. The experimental results and their analysis are discussed in Sec. IV.

II. PAIR SPECTROSCOPY

A. NN cluster model

A simple model for the magnetic response of a DMS, when $x\leq0.1$, is the NN cluster model.[5–7] In this model all exchange interactions other than the dominant NN interaction are ignored. If each NN exchange interaction is regarded as a "bond," then any Mn ion belongs to a

cluster of Mn ions which are connected by such NN bonds. The smallest cluster consists of a single Mn ion which is not attached to any bond, i.e., no NN's. The next larger cluster consists of a pair of Mn ions which are NN's of each other, but with no other NN's. Larger clusters are triplets, quartets, etc., of NN's.[8] The magnetization of the DMS is then the sum of the magnetizations of the various clusters, each cluster being independent of all other clusters. This simple picture is expected to approximate the true magnetic response of the DMS except at low temperatures and low magnetic fields[7] where both the thermal energy k_BT and the Zeeman energy (of order $g\mu_BB$) are not large compared to $2|J_{\rm NNN}|S^2$. Here, g is the g factor of the Mn^{2+} ion, $S=\frac{5}{2}$ is the spin of the Mn ion, and B is the magnetic field. Typically, the NN cluster model is a useful first approximation even at low temperatures provided that $B \gtrsim 10$ T.

B. Energy levels for a pair

Assuming a Heisenberg interaction $-2J_{\rm NN}\mathbf{S}_1\cdot\mathbf{S}_2$ between the two NN spins in a pair, one can classify the energy levels of the pair in terms of two quantum numbers: the total spin S_T of the pair and the component m of the total spin along the magnetic field. The energy levels are then[9]

$$E=-J_{\rm NN}[S_T(S_T+1)-\tfrac{35}{2}]+g\mu_BmB\ . \qquad (1)$$

The energy levels at $B=0$ are shown in Fig. 1(a). The energy separations between adjacent levels are $2|J_{\rm NN}|$, $4|J_{\rm NN}|$, etc. These energy separations can be measured directly using inelastic neutron scattering.[10,11] The observed transitions correspond to $\Delta S_T=1$. At low temperatures, where only the ground state is populated, only the $2|J_{\rm NN}|$ transition from $S_T=0$ to $S_T=1$ is observed. At higher temperatures, where the lower excited states are also populated, transitions with energies $4|J_{\rm NN}|$ or higher may also be observed. This method of pair spectroscopy is conceptually the simplest. It yields results for $J_{\rm NN}$ with an accuracy of about 2%. Thus far, this method has only been applied to Zn compounds because of the large neutron capture cross section for the naturally abundant Cd isotope.

The transitions $\Delta S_T=1$ between adjacent levels in Fig. 1(a) were also observed in Raman scattering.[12] Both $Cd_{1-x}Mn_xS$ and $Cd_{1-x}Mn_xSe$ were studied with this method. These materials have the wurtzite structure. DMS's with the zinc-blende structure gave negative results thus far. The accuracy of the Raman results is comparable to, or better than, that for the neutron data. For technical reasons, the Raman data were actually taken at low magnetic fields.

C. High-field magnetization steps

The first method used to probe the energy levels of the pairs was based on the magnetization steps which occur at high fields and low temperatures.[6,13] The energy levels of a pair as a function of B are shown in Fig. 1(b). The Zeeman splittings of the levels with $S_T\neq0$ lead to a series of energy-level crossings at $B_1,B_2,\ldots,B_5$. At each of these fields there is a change in the ground state of the pair, which results in an increase of $|m|$ by one unit. At low temperatures (where k_BT is small compared to $2|J_{\rm NN}|$), these level crossings lead to five magnetization steps. This is shown schematically in Fig. 1(c). Once the fifth step is completed the magnetization of the pairs is saturated.

A detailed theory of the magnetization steps, based on the NN cluster model, was presented in Refs. 6, 7, 13, and 14. In this simple first-order model the magnetization steps occur at fields B_r which are given by

$$g\mu_BB_r=2|J_{\rm NN}|r\ , \qquad (2)$$

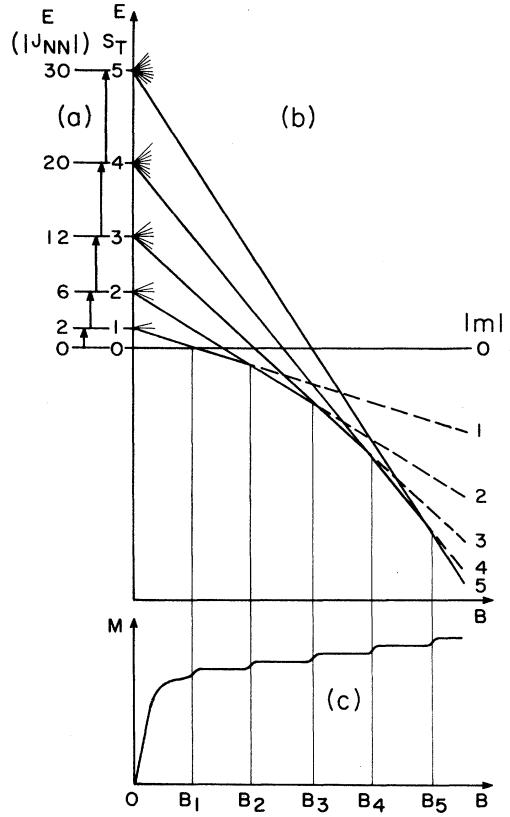

FIG. 1. (a) Upper left: energy-level diagram, in units of $|J_{\rm NN}|$, for an isolated pair of nearest-neighbor Mn^{2+} spins at zero magnetic field. Here, S_T is the total spin of the pair, E is the energy, and $J_{\rm NN}$ is the NN exchange constant. The observed transitions in inelastic neutron scattering experiments are indicated. (b) Upper right: Zeeman splitting of the energy levels as a function of magnetic field B. Note the energy-level crossings at $B_1,B_2,\ldots,B_5$. At each of these fields the ground state changes, and the magnetic moment of the ground state along **B** increases. (c) Lower trace: schematic of the magnetization M as a function of B for a dilute magnetic semiconductor at low temperatures. The five magnetization steps due to level crossings for pairs are shown. These steps are superposed on the magnetization due to spins which are not in NN pairs. The magnetization steps due to clusters larger than pairs (which are not observed as readily) are not shown.

where $r=1,2,3,4,5$. Data on various II-VI DMS's, quoted in Refs. 7 and 15, indicate that the g factor for Mn^{2+} in these materials is equal to 2.000 to within a fraction of a percent. With a typical value $J_{NN}/k_B=-10$ K, the first magnetization step occurs at ~ 15 T. Thus, only the first step (or possibly the first two steps) can normally be observed using presently available dc magnetic fields ($B \lesssim 30$ T). For this reason pulsed fields have been increasingly used for these experiments.[13,16–19]

The early determination of J_{NN} from the magnetization steps (e.g., Refs. 6 and 7) was based on the measured value of B_1 and the result from the NN cluster model

$$g\mu_B B_1 = 2|J_{NN}| \ . \tag{3}$$

However, it was subsequently discovered that Eq. (3) holds only approximately because it neglects next-nearest-neighbor exchange interactions and interactions with still more distant neighbors. The effect of these interactions on the magnetization steps was discussed by Larson, Hass, and Aggarwal.[20] Their theory leads to the result

$$g\mu_B B_r = 2|J_{NN}|r+\Delta \ , \tag{4}$$

where Δ is an energy shift due to the effective fields resulting from the distant-neighbor interactions. In the model of Larson *et al.* the shift Δ is the same for all five steps. Actually, Δ should increase slightly with increasing r, since it is roughly proportional to the magnetization M. However, the neglect of the r dependence of Δ leads to an insignificant error in J_{NN} ($<1\%$). We shall therefore take Δ to be independent of r.

If several magnetization steps are observed then the value of J_{NN} can be determined more accurately from a linear fit of the fields B_r to Eq. (4). If only the first two steps are observed, then J_{NN} is obtained from

$$g\mu_B(B_2-B_1)=2|J_{NN}| \ . \tag{5}$$

When only the first step is observed, determination of J_{NN} is of limited accuracy. In that case two options are available: (1) A rough estimate for J_{NN} can be obtained from Eq. (3). The accuracy of this estimate depends on the material, and is better for lower x. Typically, the error is less than 15% if $x<0.05$. (2) A better estimate can be made by using a procedure suggested by Barilero *et al.*[21] This procedure leads to an estimate of the shift Δ produced by more-distant-neighbor interactions, based on a fit of the shape of the magnetization curve in fields below B_1.

Using two or more steps, J_{NN} can be determined with an accuracy of about 3%. Thus far this method proved to be successful in all the DMS's which were measured in our laboratory. (The experience in other laboratories seems to be similar.) The best results are usually obtained with Mn concentrations x of several percent. Statistical considerations[6] show that at these Mn concentrations a sizable fraction of the magnetization at high fields is due to pairs. Clusters larger than pairs (e.g., open and closed triplets[8]) can also give rise to magnetization steps at high fields, but as shown in Ref. 6 these steps are much more difficult to observe. The open triplets have been observed above 35 T.[22]

III. EXPERIMENTAL TECHNIQUES

The differential susceptibility dM/dB as a function of B was determined using pulsed magnetic fields. The magnetization steps appeared as peaks in dM/dB. The fields B_r were determined from the maxima of these peaks.

A. Samples

All samples were single crystals. Samples from the same boules were previously used in similar experiments in dc magnetic fields.[7,14,15,23]

The $Zn_{1-x}Mn_xTe$ samples, with $x=0.031$ and 0.040, were grown at MIT by the traveling solvent method.[7] The $Zn_{1-x}Mn_xSe$ sample, with $x=0.033$, was obtained from Eagle-Picher Industries. It was grown from the melt. The other two samples were grown by the Bridgman method. The $Cd_{1-x}Mn_xTe$ sample, with $x=0.047$, was kindly provided by R. R. Galazka. The $Cd_{1-x}Mn_xSe$ sample, with $x=0.049$, was grown at Brown University. The Mn concentrations were determined by atomic absorption.

B. Pulsed magnets

Pulsed fields were produced by multilayer wire-wound magnets contained in a precompressed, nonmagnetic hardened-steel structures and immersed in liquid nitrogen in order to reduce resistive losses. Two types of conductors were used for the pulsed-field magnets: conventional Cu for lower fields and a new Cu/Nb metal-matrix microcomposite for higher fields. Fields up to 45 T were furnished by a 2.0-cm i.d. bore Cu wire magnet which is capable of producing a maximum field of 50 T. Fields approaching 60 T were furnished in a 1.59-cm i.d. bore Cu/Nb composite wire magnet. Recent descriptions of the performance of these magnets, and those generating fields above 68 T, are given elsewhere.[24–27] The pulsed fields were produced with a 100-kJ, 4-kV capacitor bank or with a 140-kJ, 4-kV bank. The half-periods for the Cu magnet ranged from 9.0 to 10.8 ms and that of the Cu/Nb magnet ranged from 6.3 to 7.4 ms. The waveform of the pulsed fields approximated a half-cycle of a weakly damped sine wave.

The working volumes of the magnets were somewhat restricted. That of the Cu magnet was readily accessed with a special glass liquid He Dewar which included an integral liquid N_2 section surrounding the upper section. The tail section, which was inserted in the magnet bore, was composed of a double wall of precision bore glass which had a common vacuum with the main Dewar flask. The tail section was surrounded by the liquid nitrogen in the bore of the pulsed magnet. A small pickup coil was wound on the outside of the tail section to furnish a measure of the pulsed field B. This pickup coil signal also furnished the trigger signal for the various electronic circuits. This arrangement gave adequate clearance to permit field measurement, circulation of the liquid for cool-

ing, and clearance between the tail section and the magnet insulation in the bore.

The Cu/Nb composite magnet with a 1.59-cm i.d. bore was more restrictive so that an alternative approach was used. A small liquid He Dewar with a 1.02-cm o.d. and a 0.635-cm i.d. tail section (again made with precision bore 0.5-mm wall thickness glass tubing) was used. This Dewar was surrounded by a single-wall liquid nitrogen (space-saver) type of Dewar described earlier.[28] The field pickup coil was wound on the outside of the single-wall plastic tail section of the nitrogen Dewar. Both Dewar arrangements permitted ambient bath temperatures of 1.35 K to be reached in the Dewar. As will be discussed later, although the samples were bathed in liquid He, the sample temperatures varied during the pulse because of adiabatic magnetization and demagnetization effects.

C. Detection coils

The magnetization changes were measured with a multiple-detection coil arrangement. In order to save space in the bore, an axial three-coil arrangement was used: a central coil in which the sample was positioned, and two series-opposing coils positioned above and below the central coil. The upper and lower coils each had $\frac{1}{2}$ the area turns of the central coil, in order to cancel the background signal from the pulsed field. The balance between these coils was better than 1%. A closer balance was achieved with a small additional coil whose output could be finely adjusted. The same detection coil arrangement was used for all the experiments. The sensitivity was limited by the area turns of the detection coils (which were limited by the voltage breakdown of the wire insulation), and the limits of detection coil balance which could be maintained during the pulse. At low fields a balance of about 10^{-5} was achieved. For technical reasons the balance was about 5 to 10 times worse at high fields. The output of the detection coils was fed to a differential input of a high-gain dc amplifier and preamplifier for a total gain of 10^3. A ten-bit analog-to-digital converter was used as an input to the data processing system.

The sample could be moved out of the detection coils (while maintaining a constant temperature) in order to measure the background with no sample. When background corrections were used, the background shots were taken at the same peak field as that used for the data.

D. Data acquisition and processing

Two signals were acquired during the pulse. One signal from a pickup coil was proportional to dB/dt. Later, this signal was integrated digitally to obtain B versus time t. The second (much weaker) signal was from the balanced detection coils, one of which surrounded the sample. This signal, $F(t)$, was assumed to have the form

$$F(t)=a(dM/dt)+b(t)\ , \tag{6}$$

where M is the magnetization, a is a constant, and $b(t)$ is the background. The data acquisition rate corresponded to one digitized point every 10 μs.

In many of the experiments the background $b(t)$ was obtained during the same run by measuring $F(t)$, for an identical pulse, with the sample removed. The signal $F(t)$ obtained in this manner is called the "blank-shot background." To obtain the differential susceptibility dM/dB, this background was subtracted from the "live-shot" signal $F(t)$. The difference was then divided by dB/dt. The result gave dM/dB in arbitrary units. The plot of dM/dB versus B was smoothed using a weighted average over several adjacent points, with the weights proportional to a Gaussian. This improved the signal-to-noise ratio, with a negligible effect on the positions of the steps. Typically, smoothing involved points within 10–20 % of the peak linewidth.

For some runs no blank shots were taken. The data were then processed using the same procedure except that no blank-shot background was subtracted. The resulting curve for dM/dB versus B then consisted of steps superimposed on a monotonic background. To reduce this background, a quadratic function in B was subtracted. This subtracted background will be referred to as the "analytical background," as distinguished from the blank-shot background. A single shot in a pulsed field gives results for both increasing and decreasing B. Usually, different analytical backgrounds were used for increasing and decreasing fields.

E. Temperature

The experiments were conducted with the samples immersed in liquid helium. Most pulsed-field shots were taken with the initial temperature equal to 1.4 K, but some shots were started at 2.0 K. Because the results for increasing and decreasing fields were not identical, it is believed that the temperature during the pulse was not constant. Specifically, it appears that the sample warmed during the initial portion of the pulse, where the magnetization increased rapidly. At high fields, where the magnetization varied slowly with B, the sample's temperature approached the bath temperature. Near the end of the pulse the sample's temperature was probably cooler than the bath temperature, due to the rapid demagnetization.

In most cases better data were obtained during the field-decreasing portion of the pulse. However, the values of J_{NN} deduced from the data for increasing and decreasing fields were always in agreement with each other to within the quoted uncertainties.

IV. RESULTS AND DISCUSSION

A. $Cd_{1-x}Mn_xTe$

All five magnetization steps which are predicted for pairs were observed in $Cd_{0.953}Mn_{0.047}Te$ using the 60-T magnet. An example of these data is shown in Fig. 2. This trace is for a decreasing field. A blank-shot background was used in this case.

More extensive data for this sample were taken using the 45-T magnet. With this magnet, only the first four steps could be observed. Examples of data obtained in two separate runs are shown in Fig. 3. The upper trace in Fig. 3 was obtained using a blank-shot background,

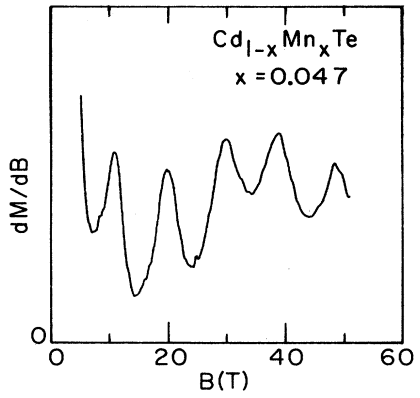

FIG. 2. Differential susceptibility dM/dB for $Cd_{0.953}Mn_{0.047}Te$ as a function of magnetic field B. These results are from the decreasing field portion of the pulse. A blank-shot background was subtracted. The initial temperature, before the pulse, was 1.4 K. Note the five peaks, corresponding to the five magnetization steps.

whereas the lower trace was obtained by subtracting an analytical background. Because the upper trace was taken at a higher temperature, the peak corresponding to the first magnetization step does not stand out as clearly as in the lower trace.

Often, the field B_r at the rth step was obtained directly from the maximum in the peak of dM/dB versus B. However, in some cases a slightly better value for B_r was obtained by subtracting a "local background." For example, the first peak in the upper trace of Fig. 3 is superimposed on a monotonic variation of dM/dB versus B. This monotonic variation was approximated by the straight line connecting the troughs on both sides of the peak, and was subtracted. The field B_1 was determined after this subtraction.

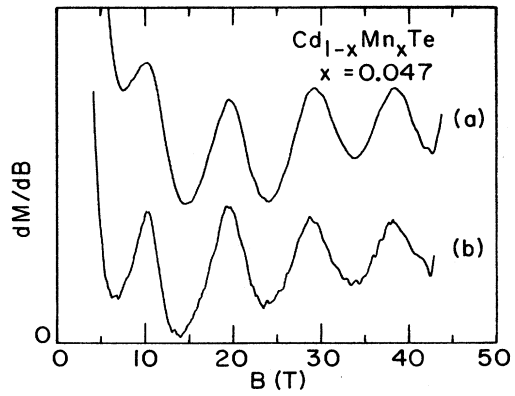

FIG. 3. Differential susceptibility dM/dB for $Cd_{0.953}Mn_{0.047}Te$ measured in decreasing fields. (a) Results with an initial temperature of 2.0 K, and with a blank-shot background subtracted. (b) Results with an initial temperature of 1.4 K, and with an analytical background subtracted. For clarity, the two traces are displaced relative to each other in the vertical direction.

The NN exchange constant J_{NN} was determined from the fields B_r using a least-squares linear fit to Eq. (4). The results for all traces were consistent, and they gave $J_{NN}/k_B = -6.2 \pm 0.2$ K. The quoted uncertainty includes the uncertainty in the field calibration. The present value for J_{NN} agrees with the value -6.1 K obtained from two steps in five dc fields.[15,23]

The trace in Fig. 2 and the upper trace in Fig. 3 (both based on a blank-shot background) show that the troughs between the third and the fourth peaks, and possibly also between the fourth and fifth peaks, are higher than the preceding troughs. A possible reason for this is the existence of unresolved magnetization steps arising from open triplets. As discussed in Ref. 6, the open triplets should give rise to five magnetization steps at $g\mu_B B/|J_{NN}| = 7, 9, 11, 13, 15$. Thus, the first of these steps should be between the third and fourth steps due to pairs.[22] The expected size of the steps due to open triplets, in the present case, is about 25% of the size of the dominant steps due to pairs. It is therefore difficult to resolve the steps due to the open triplets. Nevertheless, they may give rise to a "background" which raises the troughs between the observed steps at the highest fields.

B. $Zn_{1-x}Mn_xSe$

The magnetization steps in $Zn_{0.967}Mn_{0.033}Se$ were studied using the 45-T magnet. Some of the results (obtained using a blank-shot background) are shown in Fig. 4. Two peaks, corresponding to the first two magnetization steps, are observed for both increasing and decreasing fields. Other features which are characteristic of pulsed fields data are also noteworthy. First, there is a substantial difference at low fields between the results in increasing and decreasing fields, i.e., the large initial drop in dM/dB occurs at higher fields when the field is increasing. This means that the rapid rise of the magnetization at low fields [see Fig. 1(c)] is slower for increasing fields. This feature was also observed in other similar experiments with pulsed fields.[13,29] The most likely cause of this hys-

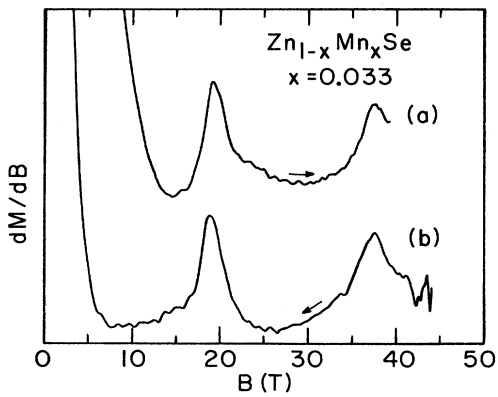

FIG. 4. Differential susceptibility dM/dB for $Zn_{0.967}Mn_{0.033}Se$. The upper curve is for increasing fields, and the lower for decreasing fields. The initial temperature was 1.4 K. A blank-shot background was subtracted. The two traces are displaced relative to each other for clarity.

teresis is the expected variation of the sample temperature during the pulse, as discussed in Sec. III E. A second feature is the smaller signal-to-noise ratio near the very top of the field, which is shown only for the lower trace in Fig. 4. This noise is a consequence of the slow time variation of B near the top of the pulse. The signals $F(t)$ and dB/dt, and the blank-shot background are then relatively small.

Using all our data, the fields B_1 and B_2 for the first two steps are 19.0±0.2 T and 37.2±0.2 T, respectively. Equation (5) then gives $J_{NN}/k_B = -12.2\pm0.3$ K, which includes the uncertainty in the field calibration. This result, which is based on two steps, is more definitive than the earlier estimates (−13, −12.6, and −12.2 K) made by our group on the basis of measurements of the first step in dc fields.[6,15,30]

Our present value for J_{NN} differs considerably from the previous result $J_{NN}/k_B = -9.9\pm0.9$ K obtained by Lascaray *et al.* from measurements of two magnetization steps in pulsed fields up to 34 T.[17] The origin of the disagreement is the different value of B_2 obtained by these authors. However, examination of Fig. 2 of Ref. 17 reveals that only a portion (less than half) of the second step was observed in their experiments. We find excellent agreement between our value for J_{NN} and the value −12.3±0.2 K obtained by neutron diffraction.[11]

C. $Zn_{1-x}Mn_xTe$

Measurements on samples with $x = 0.031$ and 0.040 were made using the 45-T magnet. Two steps, and the beginning of the third, were observed in both samples. An example of the data is shown in Fig. 5(a). A blank-shot background was used in this case. By integrating the curve in Fig. 5(a), the variation of M with B at high fields was obtained and is shown in Fig. 5(b).

The exchange constant J_{NN} was determined using B_1, B_2, and Eq. (5). The results for both samples were in good agreement. They gave $J_{NN}/k_B = -9.0\pm0.2$ K. We now compare this value with earlier results.

Several values for J_{NN} were obtained from the first magnetization step: −10.0±0.8 K (Ref. 7), −10.1±0.4 K (Ref. 31), and −9.25±0.3 K (Ref. 21). The first two values, which were the earliest, were based on Eq. (3). This equation overestimates J_{NN} because it neglects distant-neighbor interactions. The third value (the lowest) was based on an estimate of the distant-neighbor correction Δ in Eq. (4). To improve on this estimate one needs more than a single step.

Two magnetization steps, and the beginning of the third, were observed by Lascaray *et al.*[18] These data gave $J_{NN}/k_B = -8.8\pm0.1$ K. Two different values for J_{NN} were obtained by neutron diffraction: −8.79±0.14 K by Corliss *et al.*[10] and −9.5±0.2 K by Giebultowicz *et al.*[11] Our result for J_{NN} is somewhat closer to that of Corliss *et al.* and is in good agreement with the result of Lascaray *et al.*

D. $Cd_{1-x}Mn_xSe$

The first two steps were clearly observed in a sample with $x = 0.049$. They occurred at 12.8 and 24.1 T. The second step was broader than the first. This will be discussed in a subsequent publication. From the values of B_1 and B_2 we obtained $J_{NN}/k_B = -7.6\pm0.2$ K. This result is an excellent agreement with the value −7.5±0.3 K obtained from an observation of the first two steps in dc fields using Raman scattering,[23] and is also consistent with the value −7.9±0.5 K obtained by Larson *et al.*[20] from an analysis of the data in Ref. 13. A value of $J_{NN} = -8.1\pm0.2$ K was reported by Bartholomew *et al.*, based on Raman scattering from pairs.[12] A summary of various results for J_{NN} is given in Table I.

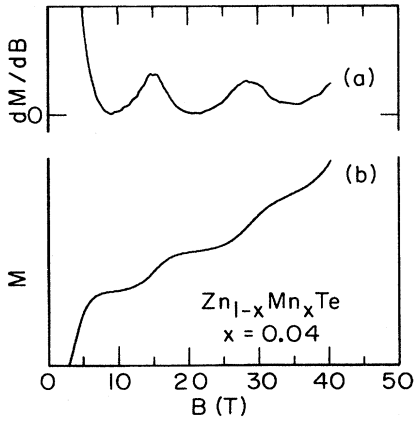

FIG. 5. (a) Differential magnetization dM/dB for $Zn_{0.96}Mn_{0.04}Te$, measured in decreasing fields. The initial temperature was 1.4 K. A blank-shot background was subtracted. (b) Magnetization M vs field B, as obtained by integrating the trace in part (a).

TABLE I. Comparison of nearest-neighbor exchange constants, J_{NN}, for $Cd_{1-x}Mn_xTe$, $Zn_{1-x}Mn_xSe$, $Zn_{1-x}Mn_xTe$, and $Cd_{1-x}Mn_{1-x}Se$ with earlier published data. All values are for small x. Data in parentheses were obtained from a single magnetization step with no correction for Δ.

Material	J_{NN}/k_B (K)	Reference
$Cd_{1-x}Mn_xTe$	−6.2 ±0.2	This work
	−6.1±0.2	15,23
$Zn_{1-x}Mn_xSe$	−12.2 ±0.3	This work
	−12.3 ±0.2	11
	−9.9 ±0.9	17
	(−13)	6
	(−12.6)	15
$Zn_{1-x}Mn_xTe$	−9.0 ±0.2	This work
	−9.25±0.3	21
	−8.8 ±0.1	18
	−8.79±0.14	10
	−9.5 ±0.2	11
	(−10.0 ±0.8)	7
	(−10.1 ±0.4)	31
$Cd_{1-x}Mn_xSe$	−7.6 ±0.2	This work
	−7.5 ±0.3	23
	−7.9 ±0.5	20
	−8.1 ±0.2	12

ACKNOWLEDGMENTS

We wish to thank R. R. Galazka for kindly providing the $Cd_{1-x}Mn_xTe$ sample, and J. Conlon and V. Diorio for valuable technical assistance. This work was partially supported by the National Science Foundation (NSF) under Grant Nos. 8504366 and DMR887419, and by the U.S. Defense Advanced Research Projects Agency (DARPA) under Grant No. N00014-86-0760. The work at Tufts University was supported by the NSF under Grant No. DMR-8900419. The work at Brown University was supported by the NSF under Grant No. DMR-8601345. The Francis Bitter National Magnet Laboratory is supported by the National Science Foundation.

[1]J. K. Furdyna, J. Appl. Phys. **64**, R29 (1988). See also J. K. Furdyna and N. Samarth, J. Appl. Phys. **61**, 3526 (1987). Various properties of DMS's are reviewed in *Diluted Magnetic Semiconductors,* Vol. 25 of *Semiconductors and Semimetals,* edited by J. K. Furdyna and J. Kossut (Academic, New York, 1988), and in *Diluted Magnetic (Semimagnetic) Semiconductors,* edited by R. L. Aggarwal, J. K. Furdyna, and S. von Molnar (Materials Research Society, Pittsburgh, 1988).

[2]B. E. Larson, K. C. Hass, and H. Ehrenreich, Phys. Rev. B **37**, 4137 (1988); **38**, 7842E (1988).

[3]A. Lewicki, J. Spalek, J. K. Furdyna, and R. R. Galazka, Phys. Rev. B **37**, 1860 (1988).

[4]T. M. Giebultowicz, J. J. Rhyne, W. Y. Ching, D. L. Huber, and R. R. Galazka, J. Magn. Magn. Mater. **54–57**, 1149 (1986).

[5]S. Nagata, R. R. Galazka, D. P. Mullin, H. Akbarzadeh, G. D. Khattak, J. K. Furdyna, and P. H. Keesom, Phys. Rev. B **22**, 3331 (1980).

[6]Y. Shapira, S. Foner, D. H. Ridgley, K. Dwight, and A. Wold, Phys. Rev. B **30**, 4021 (1984).

[7]Y. Shapira, S. Foner, P. Becla, D. N. Domingues, M. J. Naughton, and J. S. Brooks, Phys. Rev. B **33**, 356 (1986).

[8]There are two types of triplets (closed and open), and several types of quartets. The triplets are discussed in Refs. 5, 6, and 9.

[9]M. K. Kreitman, F. J. Milford, R. P. Kenan, and J. G. Daunt, Phys. Rev. **144**, 367 (1966).

[10]L. M. Corliss, J. M. Hastings, S. M. Shapiro, Y. Shapira, and P. Becla, Phys. Rev. B **33**, 608 (1986).

[11]T. M. Giebultowicz, J. J. Rhyne, and J. K. Furdyna, J. Appl. Phys. **61**, 3537 (1987).

[12]D. U. Bartholomew, E.-K. Suh, S. Rodriguez, A. K. Ramdas, and R. L. Aggarwal, Solid State Commun. **62**, 235 (1987).

[13]R. L. Aggarwal, S. N. Jasperson, Y. Shapira, S. Foner, T. Sakakibara, T. Goto, N. Miura, K. Dwight, and A. Wold, in *Proceedings of the 17th International Conference on the Physics of Semiconductors, San Francisco, 1984,* edited by J. D. Chadi and W. A. Harrison (Springer, New York, 1985), p. 1419.

[14]R. L. Aggarwal, S. N. Jasperson, P. Becla, and R. R. Galazka, Phys. Rev. B **32**, 5132 (1985).

[15]Y. Shapira and N. F. Oliveira, Jr., Phys. Rev. B **35**, 6888 (1987).

[16]N. Yamada, S. Takeyama, T. Sakakibara, T. Goto, and N. Miura, Phys. Rev. B **34**, 4121 (1986).

[17]J. P. Lascaray, M. Nawrocki, J. M. Broto, M. Rakoto, and M. Demianiuk, Solid State Commun. **61**, 401 (1987).

[18]J. P. Lascaray, A. Bruno, M. Nawrocki, J. M. Broto, J. C. Ousset, S. Askenazi, and R. Triboulet, Phys. Rev. B **35**, 6860 (1987).

[19]R. R. Galazka, W. Dobrowlski, J. P. Lascaray, M. Nawrocki, A. Bruno, J. M. Broto, and J. C. Ousset, J. Magn. Magn. Mater. **72**, 174 (1988).

[20]B. E. Larson, K. C. Hass, and R. L. Aggarwal, Phys. Rev. B **33**, 1789 (1986).

[21]G. Barilero, C. Rigaux, Nguyen Hy Hau, J. C. Picoche, and W. Giriat, Solid State Commun. **62**, 345 (1987).

[22]A clear indication of the magnetization due to open triplets has been observed by Faraday rotation in pulsed fields in (Cd,Mn)Te; X. Wang, D. Heiman, S. Foner, Y. Shapira, and P. Becla (unpublished).

[23]E. D. Isaacs, D. Heiman, P. Becla, Y. Shapira, R. Kershaw, K. Dwight, and A. Wold, Phys. Rev. B **38**, 8412 (1988).

[24]S. Foner, Appl. Phys. Lett. **49**, 982 (1986).

[25]S. Foner and E. Bobrov, in *Megagauss Technology and Pulsed Power Applications,* edited by C. M. Fowler, R. S. Caird, and D. J. Erickson (Plenum, New York, 1987), p. 31.

[26]S. Foner, E. Bobrov, C. Renaud, E. Gregory, and J. Wong, IEEE Trans. Magn. **24**, 1059 (1988).

[27]S. Foner (unpublished).

[28]S. Foner, Rev. Sci. Instrum. **40**, 1362 (1969).

[29]D. Heiman (unpublished).

[30]The estimate -13 K in Ref. 6 was based on Eq. (3). The estimate -12.6 K in Ref. 15 was based on the same equation, but used more accurate data. The estimate -12.2 K was based on the latter data and the improved procedure suggested in Ref. 21.

[31]R. L. Aggarwal, S. N. Jasperson, P. Becla, and J. K. Furdyna, Phys. Rev. B **34**, 5894 (1986).